

Freeze-out conditions in proton-proton collisions at the highest energies available at the BNL Relativistic Heavy Ion Collider and the CERN Large Hadron Collider

Sabita Das,^{1,2,*} Debadeepti Mishra,^{2,†} Sandeep Chatterjee,^{2,‡} and Bedangadas Mohanty^{2,§}

¹*Institute of Particle Physics and Key Laboratory of Quark & Lepton Physics (MOE), Central China Normal University, Wuhan 430079, China*

²*School of Physical Sciences, National Institute of Science Education and Research, HBNI, Jatni 752050, India*

(Received 7 July 2016; revised manuscript received 4 December 2016; published 24 January 2017)

The freeze-out conditions in proton-proton collisions at $\sqrt{s_{NN}} = 200, 900,$ and 7000 GeV have been extracted by fits to the mean hadron yields at midrapidity within the framework of the statistical model of an ideal gas of hadrons and resonances in the grand canonical ensemble. The variation of the extracted freeze-out thermal parameters and the goodness of the fits with $\sqrt{s_{NN}}$ are discussed. We find the extracted temperature and baryon chemical potential of the freeze-out surface to be similar in $p + p$ and heavy-ion collisions. On the other hand, the thermal behavior of the strange hadrons is qualitatively different in $p + p$ as compared to $A + A$ collisions. We find an additional parameter accounting for nonequilibrium strangeness production is essential for describing the $p + p$ data. This is in contrast to $A + A$ where the nonequilibrium framework could be successfully replaced by a sequential and complete equilibrium model with an early freeze-out of the strange hadrons.

DOI: [10.1103/PhysRevC.95.014912](https://doi.org/10.1103/PhysRevC.95.014912)

I. INTRODUCTION

The statistical model of noninteracting gas of hadrons and resonances at some volume V , temperature T , and conserved charge chemical potentials μ_B , μ_Q , and μ_S , corresponding to the three conserved charges of QCD, namely baryon number B , electric charge Q , and strangeness S , has been remarkably successful in providing a good qualitative description of the mean hadron yields in heavy-ion collision experiments across a wide range of beam energies available at the BNL Alternating Gradient Synchrotron (AGS) to the CERN Large Hadron Collider (LHC) [1–3]. This could possibly indicate a hadronic medium in thermal equilibrium prior to freeze-out. However, the extracted thermal parameters indicate that the freeze-out surface lies very close to the hadronization surface [4,5]. This has led to the suggestion that the hadrons are directly born into equilibrium from the quark-gluon plasma (QGP) phase instead of there being a microscopic collision mechanism for equilibration [6]. A microscopic collision picture has been suggested by invoking contributions from Hagedorn resonances with exponential mass spectrum [7]. Recently, in yet another approach based on Unruh radiation, a universal freeze-out temperature was suggested for systems starting from $e + e$ and $p + p$ to heavy ions [8]. Thus, despite the enormous phenomenological success of the thermal models, the microscopic understanding of such fast thermal equilibration is still an open question.

One crucial ingredient in the application of thermal models is the choice of the ensemble to treat the conserved charges. Ideally, conserved charges in an open system should be treated within a grand canonical ensemble (GCE) while

those in a closed system should be treated canonically. Thus, 4π data should be treated canonically while, for midrapidity measurements that represent an open system, grand canonical ensembles should be applicable. However, it is not so straightforward in the case of particle production in relativistic collisions. It is believed that even if the criteria for applicability of a GCE, $VT^3 > 1$, holds true for the bulk of the produced particles, canonical suppression might still be required when the number of carriers of a specific conserved charge are few [9]. For this reason, strangeness has been treated canonically in $p + p$ collisions owing to the small system size for the $\sqrt{s_{NN}} = 200$ GeV midrapidity data at the BNL Relativistic Heavy Ion Collider (RHIC) [9].

It is interesting to test the framework of thermal models in small systems [10,11]. Previously, thermal models have been used to describe particle yields in small systems with a fair degree of success [9,10,12–14]. It is a commonly accepted notion that in small systems the formation of a thermally equilibrated fireball through multiple scattering of its constituents is less likely than in $A + A$ collisions. However, it has been demonstrated through explicit application of thermal models that the quality of description of the data is similar for different system sizes [15].

In this article, we apply the thermal model on midrapidity data in $p + p$ collisions at $\sqrt{s_{NN}} = 200$ (RHIC), 900 (LHC), and 7000 (LHC) GeV. We find the midrapidity data is described by the GCE at all the above $\sqrt{s_{NN}}$. A comparative study of two different schemes of treating the strange hadrons in $p + p$ collisions—either having a strangeness correlation volume different from the fireball volume or using a strangeness under-saturation factor γ_S —yielded similar goodness of fits for both the schemes [10]. We have kept the strangeness conservation volume equal to the fireball volume, allowing nonequilibrium strangeness production only through the departure from unity of γ_S . At the energies available at the LHC we have fixed the chemical potentials to zero.

*sabita@rcf.rhic.bnl.gov

†debadeepti.m@niser.ac.in

‡sandeepc@niser.ac.in

§bedanga@niser.ac.in

TABLE I. Details of the data sets used for fit with references.

| $\sqrt{s_{NN}}$ (GeV) | Expt. | System | Particle yields (dN/dy) | Antiparticle yields (dN/dy) | Ref. |
|-----------------------|-------|----------------------------|---|---|------|
| 200 | STAR | $p + p$ | π^+ : 1.44 ± 0.11 | π^- : 1.42 ± 0.11 | [17] |
| | | | K^+ : 0.150 ± 0.013 | K^- : 0.145 ± 0.013 | [17] |
| | | | p : 0.138 ± 0.012 | \bar{p} : 0.113 ± 0.010 | [17] |
| | | | Λ : 0.0385 ± 0.0036 | $\bar{\Lambda}$: 0.0351 ± 0.0033 | [18] |
| | | | Ξ^- : 0.0026 ± 0.0009 | $\bar{\Xi}^+$: 0.0029 ± 0.001 | [18] |
| | | | K_S^0 : 0.134 ± 0.011 | | [18] |
| | | | $\Omega + \bar{\Omega}$: 0.00034 ± 0.00019 | | [18] |
| | | ϕ : 0.018 ± 0.003 | | [19] | |
| 900 | ALICE | $p + p$ | π^+ : 1.493 ± 0.0741 | π^- : 1.485 ± 0.0741 | [20] |
| | | | K^+ : 0.183 ± 0.0155 | K^- : 0.182 ± 0.0155 | [20] |
| | | | p : 0.083 ± 0.0063 | \bar{p} : 0.079 ± 0.0063 | [20] |
| | | | Λ : 0.048 ± 0.0041 | $\bar{\Lambda}$: 0.047 ± 0.0054 | [21] |
| | | | $\Xi^- + \bar{\Xi}^+$: 0.0101 ± 0.0022 | | [21] |
| | | | K_S^0 : 0.184 ± 0.0063 | | [21] |
| | | | ϕ : 0.021 ± 0.005 | | [21] |
| 7000 | ALICE | $p + p$ | π^+ : 2.26 ± 0.1 | π^- : 2.23 ± 0.1 | [22] |
| | | | K^+ : 0.286 ± 0.016 | K^- : 0.286 ± 0.016 | [22] |
| | | | p : 0.124 ± 0.009 | \bar{p} : 0.123 ± 0.01 | [22] |
| | | | Ξ^- : 0.008 ± 0.000608 | $\bar{\Xi}^+$: 0.0078 ± 0.000608 | [23] |
| | | | Ω : 0.00067 ± 0.000085 | $\bar{\Omega}$: 0.00068 ± 0.000085 | [23] |
| | | | ϕ : 0.032 ± 0.004 | | [24] |

II. THERMAL MODEL

In a single chemical freeze-out scheme (1CFO) all the hadrons freeze-out from the same surface characterised by $(V, T, \mu_B, \mu_Q, \mu_S)$. The particle multiplicities become

$$N_i = \frac{g_i V}{2\pi^2} \sum_{k=1}^{\infty} (\pm 1)^{k+1} \frac{m_i^2 T}{k} K_2\left(\frac{km_i}{T}\right) \exp(\beta k \mu_i) \gamma_S^{k|S_i|}, \quad (1)$$

where V is the fireball volume, g_i is the degeneracy, m_i is the particle mass, and K_2 is a second-order Bessel function. $\beta = \frac{1}{T}$, where T is the chemical freeze-out temperature. The plus sign is for bosons and the minus sign is for fermions. The hadron chemical potential μ_i in the case of complete chemical equilibrium can be written down in terms of μ_B , μ_Q , and μ_S as follows:

$$\mu_i = B_i \mu_B + Q_i \mu_Q + S_i \mu_S, \quad (2)$$

where B_i , Q_i , and S_i are the baryon number, the charge, and the strangeness of the i th hadron. It is a standard practice to extract μ_S and μ_Q from the following constraints:

$$\text{Net}S = 0, \quad (3)$$

$$\text{Net}B/\text{Net}Q = 1. \quad (4)$$

Equation (4) is valid only for $p + p$ collisions. In $A + A$ collisions, the unity in the right-hand side of Eq. (4) should be replaced by ~ 2.5 . The remaining parameters (V, T, μ_B) are extracted from fits to hadron yields. The total yield N_i^{tot} of the i th hadron includes primordial yields (produced directly in the reaction) and secondary yields which are the feed-down from

the decays of heavier resonances:

$$N_i^{\text{tot}} = N_i^{\text{prim}} + \sum_{\text{states } j} N_j^{\text{prim}} \text{BR}(j \rightarrow i), \quad (5)$$

where N_i^{prim} is the primordial multiplicity of species i and $\text{BR}(j \rightarrow i)$ is the branching ratio of j to i through all possible channels. We have used the THERMUS code [16], which is available publicly, for the 1CFO analysis.

As seen in Eq. (1), there is one more parameter, γ_S , which is also treated as a free parameter and extracted from fits to data. It accounts for possible chemical nonequilibrium of strangeness in the fireball. In a complete equilibrium scenario, $\gamma_S = 1$.

III. DATA SETS

We have used the $p + p$ collision midrapidity data sets at the RHIC with $\sqrt{s_{NN}} = 200$ GeV [17–19] and at the LHC with $\sqrt{s_{NN}} = 900$ GeV [20,21] and 7 TeV [22–24]. The π^\pm and Λ are feed-down corrected from weak decays, whereas (anti)protons at the RHIC are inclusive. The data sets from the LHC have π^\pm , p , \bar{p} , and Λ that are feed-down corrected from weak decays. The details about the data sets used in this study are given in Table I.

IV. RESULTS

In Fig. 1 we have plotted the fitted freeze-out parameters obtained in GCE in the 1CFO scheme. Previously, the RHIC $\sqrt{s_{NN}} = 200$ GeV $p + p$ midrapidity data (excluding ϕ) has been fitted in the strangeness canonical ensemble [9]. However, we find here that the GCE provides reasonable description with $\chi^2/\text{ndf} \sim 1-2$ even when including ϕ . The thermal model results for the midrapidity LHC data at $\sqrt{s_{NN}} = 900$ and

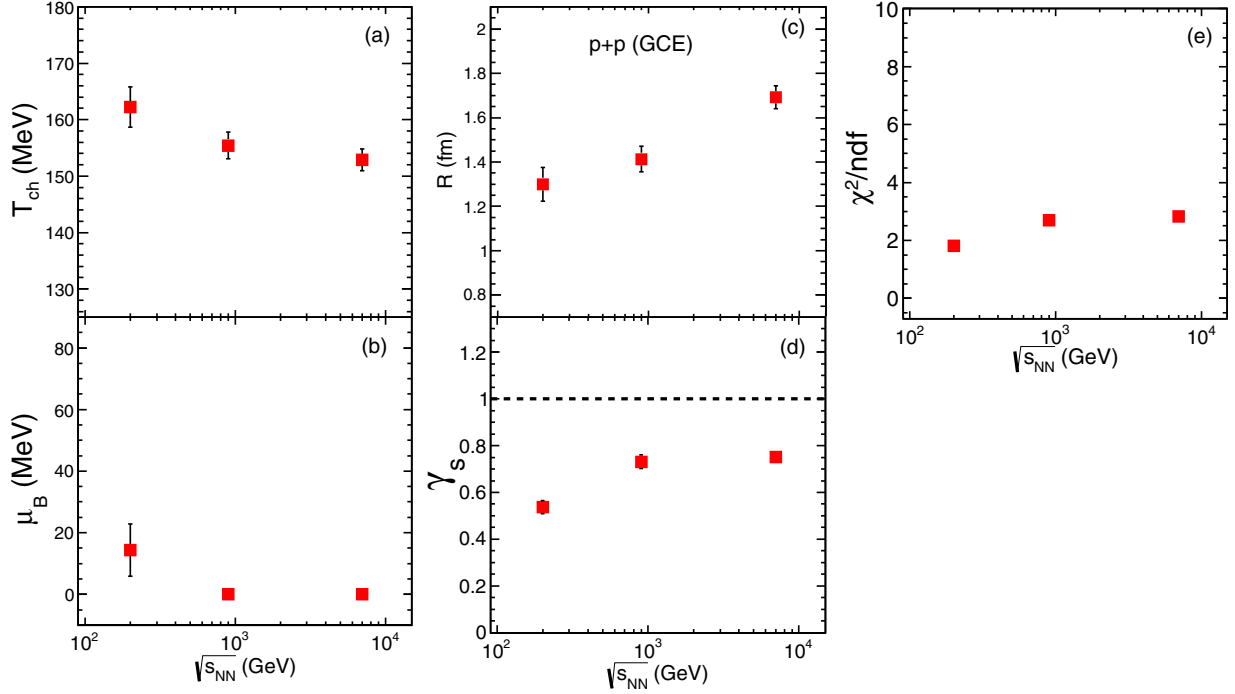


FIG. 1. Freeze-out parameters T_{ch} , μ_B , γ_S , R , and χ^2/ndf obtained from a statistical model fit [16] using midrapidity particle yields.

7000 GeV are new. The χ^2/ndf value is around 2–3 which has marginally increased from the highest energy available at the RHIC. The obtained freeze-out parameters along with the χ^2 of the fits are tabulated in Table II.

The value of γ_S monotonically rises from 0.6 to 0.8 between the energies available at the RHIC and the LHC. The freeze-out T on the other hand monotonically decreases from 160 MeV at $\sqrt{s_{NN}} = 200$ GeV to ~ 150 MeV at $\sqrt{s_{NN}} = 7$ TeV. The fireball radius rises from ~ 1.3 fm at $\sqrt{s_{NN}} = 200$ GeV to ~ 1.7 fm at $\sqrt{s_{NN}} = 7$ TeV. μ_B is relatively flat and hovers around zero.

Earlier, we had noted that the χ^2/ndf value marginally rises from the highest energies available at the RHIC to the highest energies available at the LHC. A rise in the χ^2/ndf values does not necessarily mean a worsening of the thermal model fits. It could also occur due to more precise measurements. This could be verified by comparing the deviation between the model and the data defined as

$$\text{deviation} = \frac{\text{data} - \text{model}}{\text{data}}. \quad (6)$$

Figures 2(a) and 2(b) show the deviation for $\sqrt{s_{NN}} = 200$ and 7000 GeV, respectively. At 7000 GeV, the deviations

TABLE II. The chemical freeze-out parameters extracted in 1CFO scheme in GCE at $\sqrt{s_{NN}} = 200, 900$ and 7000 GeV.

| $\sqrt{s_{NN}}$ (GeV) | T (MeV) | μ_B (MeV) | γ_S | R (fm) | $\chi^2/$ ndf |
|--------------------------|-----------------|----------------|-----------------|-----------------|--------------------|
| 200 | 162.2 ± 3.6 | 14.4 ± 8.5 | 0.54 ± 0.03 | 1.3 ± 0.08 | 16.3 / 1.8 |
| 900 | 155.4 ± 2.4 | 0.0 (Fixed) | 0.73 ± 0.03 | 1.42 ± 0.06 | 27.0 / 2.7 |
| 7000 | 152.9 ± 2.0 | 0.0 (Fixed) | 0.75 ± 0.02 | 1.69 ± 0.05 | 22.6 / 2.8 |

between the data and the model for all the hadron species are within 20%. Even at 200 GeV, we find that, except for Ω and ϕ , the deviation for the rest of the hadrons are all within 20%. This shows clearly that the rise in χ^2/ndf values from the energies available at the RHIC to the energies available at the LHC is due to more precision measurements at the LHC. Further, in Fig. 2(a) we have also compared the deviation for each species between $p + p$ and heavy-ion collisions (HICs) for $\sqrt{s_{NN}} = 200$ GeV. We find that the hadrons with multiple valence strange quarks like ϕ , Ξ , and Ω show higher deviations in $p + p$ cases compared to HICs.

Finally, we have compared in Fig. 3 the freeze-out parameters T , μ_B , γ_S , and R extracted in HICs with that of $p + p$ collision in the 1CFO scheme. At lower $\sqrt{s_{NN}}$, the $p + p$ freeze-out T is higher than that in $A + A$ as was recently reported [14]. However at higher beam energies ($\sqrt{s_{NN}} > 200$ GeV), the T extracted from $p + p$ collisions is in agreement with that from HICs. As we go from energies available at the RHIC to energies available at the LHC, both $p + p$ and $A + A$ collisions show a decrease of the freeze-out temperature by about 10 MeV. μ_B extracted from $p + p$ collisions is similar to that obtained from $A + A$ collisions. γ_S and R are quite different in the two systems. Between the highest energies available at the SPS and the LHC, while the R in $A + A$ collisions doubles, the corresponding rise in $p + p$ collisions is only about 20%. In this entire range, the radius in $p + p$ collisions is almost 5–10 times smaller compared to that in $A + A$ collisions. In $A + A$ collisions, γ_S is consistent with unity while in $p + p$ collisions it is around 0.2 at the SPS and then steadily rises before saturating around 0.8 at the LHC. This indicates significant strangeness suppression in $p + p$ collisions as compared to heavy-ion collisions even

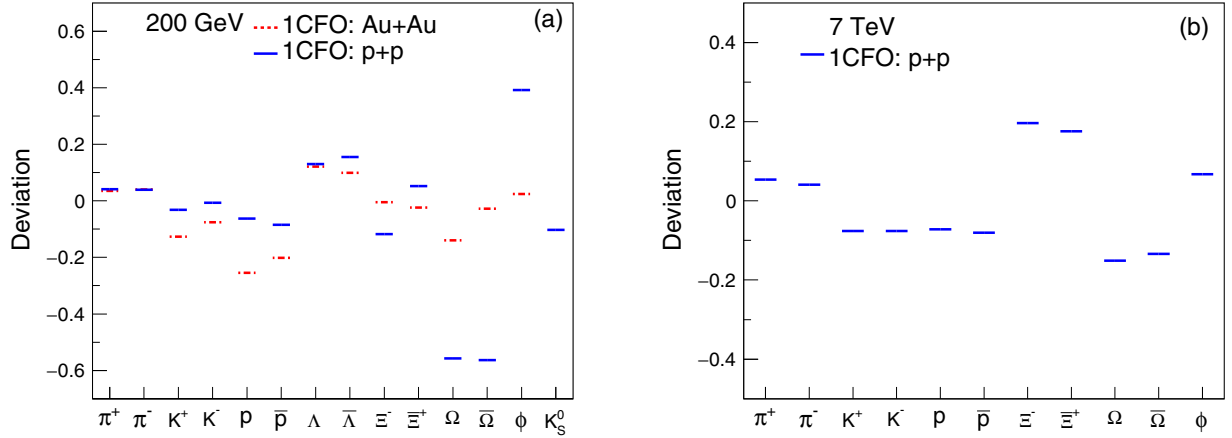


FIG. 2. (a) The deviation between model and data for each species in the 1CFO scheme at $\sqrt{s_{NN}} = 200$ GeV compared between $p + p$ and heavy-ion collisions. (b) The deviation between model and data in the 1CFO scheme at $\sqrt{s_{NN}} = 7$ TeV.

at energies available at the LHC. It will be interesting to see whether at even higher beam energies we produce strangeness in complete equilibrium or not. In this regard we note from Fig. 2 that in $p + p$ collisions there is large deviation between

the data and the model as compared to heavy-ion collisions for hadrons with multiple strange valence quarks.

The recent data from Pb + Pb collisions at $\sqrt{s_{NN}} = 2.76$ TeV have renewed the interest in thermal models because

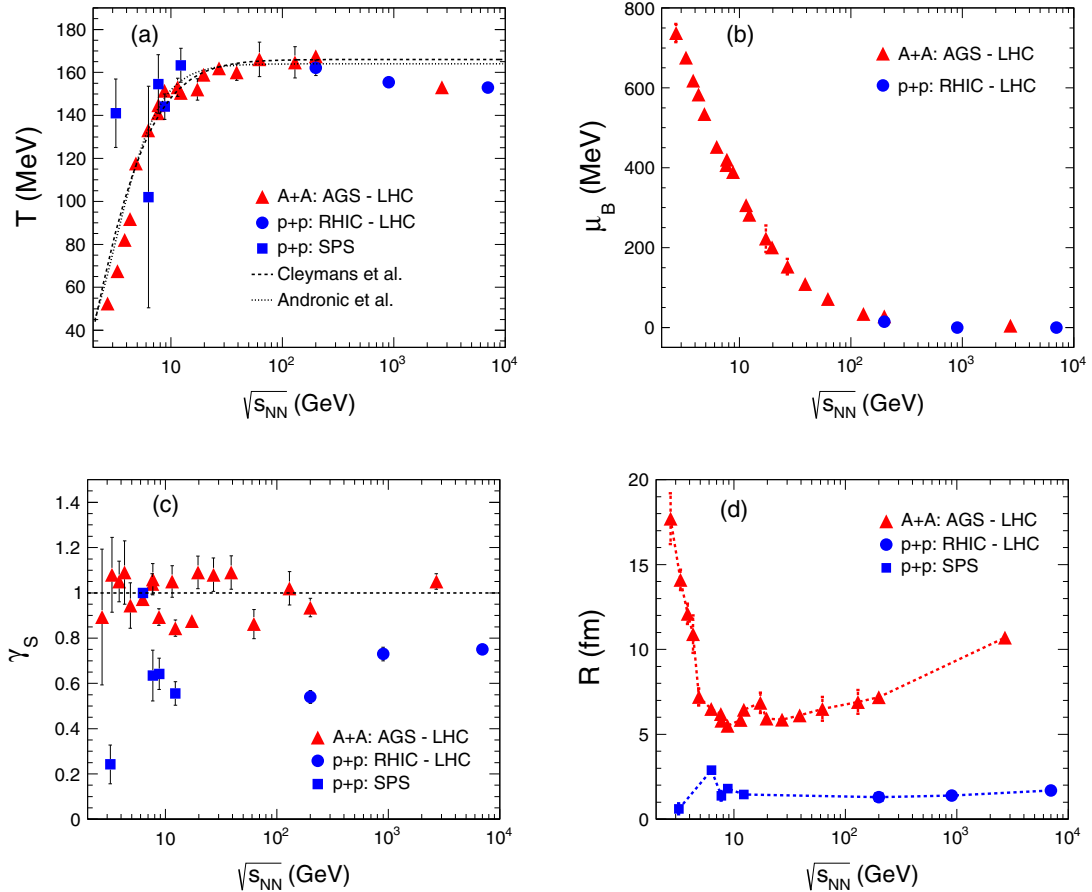


FIG. 3. A compilation of T (a), μ_B (b), γ_S (c), and R (d) vs $\sqrt{s_{NN}}$ in $p + p$ collisions shown by blue squares for energies available at the CERN Super Proton Synchrotron (SPS) taken from Ref. [14] and by blue circles for energies available at the RHIC and the LHC, which are the results of this paper. The results for $A + A$ are shown by red triangles for comparison [3]. The T vs $\sqrt{s_{NN}}$ parametrizations shown by dashed lines are from Refs. [25] and [26].

the standard 1CFO freeze-out scheme failed to explain the data satisfactorily, with a notable disparity between model and experiment in the proton to pion ratio, commonly known as the proton anomaly [27,28]. Several alternative freeze-out schemes have been proposed to address the above issue [29–32]. One of them is the two freeze-out scheme (2CFO) where those hadrons with nonzero strangeness content are allowed to freeze-out at a different surface as compared to those with zero strangeness [31,32]. The 2CFO scheme has successfully described the proton anomaly [31] and transverse momentum spectra [33] at the LHC, the ${}^3_{\Lambda}\text{H}/{}^3\text{He}$ ratio at $\sqrt{s_{NN}} = 200$ GeV, and the $\bar{\Lambda}/\bar{p}$ ratio at lower beam energies which cannot be described by the 1CFO scheme [3,34]. We have checked the above $p + p$ data in the 2CFO scheme as well. However, unlike in HICs where the 2CFO scheme provides a much better description of the hadron yields than the 1CFO scheme [31], here in $p + p$ collisions we find the χ^2/ndf value is similar and one does not gain much by introducing two additional parameters in 2CFO compared to γ_s augmented 1CFO. Thus in $p + p$ collisions, the 1CFO scheme with the additional strangeness suppression factor γ_s seems to be a better scheme than the complete chemical equilibrium but sequential freeze-out scheme of 2CFO. The primary motivation for a 2CFO scheme in $A + A$ collisions is the expected flavor hierarchy in hadron-hadron cross sections, which results in different flavored hadrons freezing out at different times. However, in $p + p$ collisions hadronic interactions are much reduced and the quick expansion results in a rapid freeze-out, leaving little room for sequential freeze-out to occur.

V. SUMMARY

The freeze-out conditions for $p + p$ collisions were extracted from the data on hadron yields at midrapidity for $\sqrt{s_{NN}} = 200, 900, \text{ and } 7000$ GeV. Previous analyses have

mostly focused on a canonical treatment of strangeness in $p + p$ collisions irrespective of the detector acceptance. We performed the analysis in the grand canonical ensemble because it is expected to describe the midrapidity system that behaves like an open system.

At these highest beam energies, while the extracted temperature and baryon chemical potential are in agreement with those from heavy-ion collisions, the strangeness suppression factor comes out to be ~ 0.8 in $p + p$ collisions. Thus the main difference arises in the freeze-out condition for the strange hadrons. In $A + A$ collisions, a complete thermal and chemical equilibrium scheme with early freeze-out for strangeness provides a good description of the data. However, here in $p + p$ collisions we found that a single freeze-out scheme extended by a nonequilibrium factor for strangeness production provides the best description of the data amongst the different ensemble and freeze-out schemes. We find a strong strangeness suppression across all the beam energies—about 20% suppression is found even at the highest energies available at the LHC. The expected shorter lifetime of the fireball in the case of $p + p$ collisions could be a reason behind such difference in the freeze-out behavior of the strange hadrons.

ACKNOWLEDGMENTS

We acknowledge Jürgen Schukraft for his helpful comments on the manuscript. S.D. thanks Jean Cleymans for helpful discussions and the MoST of China 973-Project No. 2015CB856901 and the XIIth Plan Project No. 12-R&D-NIS-5.11-0300 of the Government of India for support. D.M. acknowledges the support from DAE and DST/SERB Project of the Government of India. S.C. thanks the XIIth Plan Project No. 12-R&D-NIS-5.11-0300 of the Government of India for support. B.M. acknowledges support from DST SwarnaJayanti and DAE-SRC Projects.

-
- [1] F. Becattini, J. Cleymans, A. Keranen, E. Suhonen, and K. Redlich, *Phys. Rev. C* **64**, 024901 (2001).
 - [2] A. Andronic, P. Braun-Munzinger, and J. Stachel, *Nucl. Phys. A* **772**, 167 (2006).
 - [3] S. Chatterjee *et al.*, *Adv. High Energy Phys.* **2015**, 349013 (2015).
 - [4] O. Kaczmarek, F. Karsch, E. Laermann, C. Miao, S. Mukherjee, P. Petreczky, C. Schmidt, W. Soeldner, and W. Unger, *Phys. Rev. D* **83**, 014504 (2011).
 - [5] G. Endrodi *et al.*, *J. High Energy Phys.* **04** (2011) 001.
 - [6] R. Stock, *Phys. Lett. B* **456**, 277 (1999).
 - [7] J. Noronha-Hostler, C. Greiner, and I. A. Shovkovy, *Phys. Rev. Lett.* **100**, 252301 (2008).
 - [8] P. Castorina, D. Kharzeev, and H. Satz, *Eur. Phys. J. C* **52**, 187 (2007).
 - [9] I. Kraus, J. Cleymans, H. Oeschler, and K. Redlich, *Phys. Rev. C* **79**, 014901 (2009).
 - [10] I. Kraus, J. Cleymans, H. Oeschler, K. Redlich, and S. Wheaton, *Phys. Rev. C* **76**, 064903 (2007).
 - [11] J. Cleymans *et al.*, arXiv:1603.09553.
 - [12] F. Becattini and U. Heinz, *Z. Phys. C* **76**, 269 (1997).
 - [13] I. Kraus, J. Cleymans, H. Oeschler, and K. Redlich, *Phys. Rev. C* **81**, 024903 (2010).
 - [14] V. Vovchenko, V. V. Begun, and M. I. Gorenstein, *Phys. Rev. C* **93**, 064906 (2016).
 - [15] F. Becattini, P. Castorina, A. Milov, and H. Satz, *Eur. Phys. J. C* **66**, 377 (2010).
 - [16] S. Wheaton, J. Cleymans, and M. Hauer, *Comput. Phys. Commun.* **180**, 84 (2009).
 - [17] B. I. Abelev *et al.*, *Phys. Rev. C* **79**, 034909 (2009).
 - [18] B. I. Abelev *et al.*, *Phys. Rev. C* **75**, 064901 (2007).
 - [19] B. I. Abelev *et al.*, *Phys. Rev. C* **79**, 064903 (2009).
 - [20] K. Aamodt *et al.*, *Eur. Phys. J. C* **71**, 1655 (2011).
 - [21] K. Aamodt *et al.*, *Eur. Phys. J. C* **71**, 1594 (2011).
 - [22] J. Adam *et al.*, *Eur. Phys. J. C* **75**, 226 (2015).
 - [23] B. I. Abelev *et al.*, *Phys. Lett. B* **712**, 309 (2012); E. Abbas *et al.*, *Eur. Phys. J. C* **73**, 2496 (2013).
 - [24] B. I. Abelev *et al.*, *Eur. Phys. J. C* **72**, 2183 (2012).
 - [25] J. Cleymans, H. Oeschler, K. Redlich, and S. Wheaton, *J. Phys. G* **32**, S165 (2006).
 - [26] A. Andronic, P. Braun-Munzinger, and J. Stachel, *Nucl. Phys. A* **834**, 237c (2010).

- [27] M. Rybczynski, W. Florkowski, and W. Broniowski, *Phys. Rev. C* **85**, 054907 (2012).
- [28] J. Stachel *et al.*, *J. Phys.: Conf. Ser.* **509**, 012019 (2014).
- [29] J. Steinheimer, J. Aichelin, and M. Bleicher, *Phys. Rev. Lett.* **110**, 042501 (2013).
- [30] M. Petráň, J. Letessier, V. Petráček, and J. Rafelski, *Phys. Rev. C* **88**, 034907 (2013).
- [31] S. Chatterjee, R. Godbole, and S. Gupta, *Phys. Lett. B* **727**, 554 (2013).
- [32] K. A. Bugaev *et al.*, *Europhys. Lett.* **104**, 22002 (2013).
- [33] S. Chatterjee, B. Mohanty, and R. Singh, *Phys. Rev. C* **92**, 024917 (2015).
- [34] S. Chatterjee and B. Mohanty, *Phys. Rev. C* **90**, 034908 (2014).